Integrative Biology

PAPER

View Article Online
View Journal | View Issue

Cite this: *Integr. Biol.*, 2015, 7, 1161

Oxygen governs gonococcal microcolony stability by enhancing the interaction force between type IV pili†

Lena Dewenter, Thorsten E. Volkmann and Berenike Maier*

Received 23rd January 2015,
Accepted 14th April 2015

DOI: 10.1039/c5ib00018a

www.rsc.org/ibiology

The formation of small bacterial clusters, called microcolonies, is the first step towards the formation of bacterial biofilms. The human pathogen *Neisseria gonorrhoeae* requires type IV pili (T4P) for microcolony formation and for surface motility. Here, we investigated the effect of oxygen on the dynamics of microcolony formation. We found that an oxygen concentration exceeding 3 μM is required for formation and maintenance of microcolonies. Depletion of proton motive force triggers microcolony disassembly. Disassembly of microcolonies is actively driven by T4P retraction. Using laser tweezers we showed that under aerobic conditions T4P–T4P interaction forces exceed 50 pN. Under anaerobic conditions T4P–T4P interaction is severely inhibited. We conclude that oxygen is required for gonococcal microcolony formation by enhancing pilus–pilus interaction.

Insight, innovation, integration

Oxygen affects the lifestyle within bacterial communities. Here, we show that at oxygen concentrations larger than the threshold concentration of $[O_2] = 3$ μM gonococci form clusters called microcolonies. These clusters are stably maintained and grow in size. Below the threshold concentration microcolonies disassemble. Disassembly requires active pilus retraction. Mechanistically, the interaction force between pili governs assembly and disassembly as a function of oxygen concentration. For quantifying interaction forces between pili, we developed a method for measuring the force that a single bacterium generates by pilus retraction onto other type IV pili. Furthermore, we established a method for characterizing the kinetics of assembly and disassembly of bacterial clusters while simultaneously measuring the oxygen concentration.

Department of Physics, Universität zu Köln, Köln, Germany.
E-mail: berenike.maier@uni-koeln.de

† Electronic supplementary information (ESI) available: Movie S1. Dynamics of gonococcal microcolonies. Gonococci were applied to the flow chamber and imaged at the PDMS surface with integrated oxygen sensor. In the beginning, microcolonies were present and had depleted the oxygen. At various time points fresh medium saturated with oxygen was supplied. Movie S2. Dynamics of large gonococcal microcolony. Gonococci were applied to the flow chamber and imaged at the PDMS surface with integrated oxygen sensor. In the beginning, microcolonies were present and had depleted the oxygen. At various time points fresh medium saturated with oxygen was supplied. Movie S3. Dynamics of T4P-retraction-deficient $pilT_{ind}$ gonococcal microcolonies. Gonococcal microcolonies were applied to the flow chamber and imaged at the PDMS surface with integrated oxygen sensor. At various time points fresh medium saturated with oxygen was supplied. Movie S4. Dynamics of gonococci on T4P-coated surface under aerobic conditions. Movie S5. Dynamics of gonococci on T4P-coated surface under anaerobic conditions. Movie S6. Dynamics of gonococcal microcolonies in the presence of chromosomal DNA. Gonococci were applied to the flow chamber in the presence of an excess of chromosomal DNA and imaged at the PDMS surface with integrated oxygen sensor. Fig. S1. Active T4P retraction is required for disassembly of microcolonies under anaerobic conditions. $pilT_{ind}$ gonococci with 10 mM IPTG were imaged at the PDMS surface with integrated oxygen sensor. Top: microscopic images of a typical large colony in the presence and absence of oxygen. Scale bar: 10 μm. Bottom: concentration of oxygen as a function of time. The red dashed line denotes the minimal oxygen concentration necessary for microcolony stability. Arrows denote the time points at which the images shown were taken. See DOI: 10.1039/c5ib00018a

Introduction

During the initiation of biofilms, bacteria tend to upregulate their interaction strength with surfaces and to down-regulate motility. Counterintuitively, the same surface organelles are often used for motility and attachment. For example, flagella are used for swimming motility but also for attachment to the surface.[1,2] For several systems, it is known how this conflict is solved. For example, *Bacillus subtilis* disables flagella rotation during biofilm formation by disengaging force-generating motor elements.[3] *Pseudomonas aeruginosa* switches from a swimming phenotype to a swarming behavior using flagella and type IV pili (T4P) in a coordinated fashion.[4,5] Additionally, *P. aeruginosa* confines T4P driven motility by generating networks of extracellular polysaccharides and DNA on the surface.[6–8]

Type IV pili (T4P) are multi-functional extracellular polymers.[9] Their functions include adhesion to inert surfaces and host cells, microcolony formation, surface motility, and horizontal gene transfer. The major subunit of the pilus, *pilE*,

polymerizes into helical polymers[10] with a length of ~ 1 μm.[11] The major pilin subunit is a P-shaped molecule with a hydrophobic tail that mediates polymerization and a hydrophilic head exposed to the environment.[10,12] Minor pilins modify the function of the T4P.[9,13–16] The major pilins of the human pathogens *Neisseria gonorrhoeae* (gonococci) and *Neisseria meningiditis* are associated with a system that supports antigenic variation of *pilE*.[17] Therefore the structure of *pilE* varies continuously. Moreover, post-translational modification of *pilE* affects the interaction between bacteria and their host cells.[18–20] All of these factors, namely minor pilins, post-translational modification, as well as antigenic variation are likely to determine the strength of pilus–surface and pilus–pilus interaction.

Type IV pili of *N. gonorrhoeae* and *Myxococcus xanthus* are among the strongest molecular motors with a single pilus generating more than 100 pN force.[21–23] The PilT retraction ATPase is essential for pilus retraction by depolymerization.[24,25] Cycles of T4P elongation, adhesion, and retraction mediate surface movement.[26] The movement of *N. gonorrhoeae* on inert surfaces is consistent with a tug-of-war mechanism.[11,27,28] On inert surfaces, T4P support both surface motility and microcolony formation. Confinement of motility and high cell density promote microcolony formation.[29] The T4P system is a multimodal system, *i.e.* T4P can retract in different speed modes or they can elongate.[30,31] Switching between theses modes occurs at two different time scales, either a scale of milliseconds or at a scale of hundreds of milliseconds.[30] Recently, we found that the occupation probability of these modes strongly depends on the oxygen concentration and on the external force.[32] Under aerobic conditions (and low force in the range of 10 pN), individual T4P retract at a speed of ~ 2 μm s^{-1}. Under anaerobic conditions the speed of T4P retraction is ~ 1 μm s^{-1}. The underlying mechanism of reduced retraction speed is the reduction of proton motive force.[33]

In this study, we investigated the role of oxygen on the initiation of gonococcal biofilms, namely on the formation and stability of microcolonies. We found that early microcolonies (containing $\leq$1000 bacteria) disassembled upon depletion of oxygen. Disassembly required retractile T4P. Re-assembly occurred on a timescale of seconds in response to oxygen replenishment. By measuring the interaction force between piliated gonococci and T4P in the presence and absence of oxygen we found that pilus–pilus interaction but not pilus–glass interaction was heavily reduced in the absence of oxygen. In summary, we demonstrate that oxygen is important for early biofilm formation because it impacts on pilus–pilus interaction.

Results

Oxygen depletion triggers disassembly of early gonococcal microcolonies

Our aim was to assess the influence of oxygen on the dynamics of microcolony formation. To this end, we used a microscopy flow chamber which allowed for application of bacteria and exchange of medium during image acquisition. To continuously monitor the oxygen concentration, the surface was coated with the porphyrin dye PtTFPP embedded into a layer of polydimethylsiloxane (PDMS). The phosphorescence intensity of the embedded dye is quantitatively quenched in the presence of oxygen. Using a previously described calibration method,[32] we measured the oxygen concentration while monitoring the dynamics of the microcolonies.

Gonococci were applied to the flow cell at a density that was low enough to ensure that mostly single cells adhered to the surface. Subsequently, the flow of medium was turned off. Gonococci were motile, *i.e.* they showed type IV pilus (T4P)-driven twitching motility. Motile cells formed clusters called microcolonies whose size increased by integration of motile single cells, fusion of small colonies, and by cell division. Since the medium was not exchanged and the bacteria consumed oxygen, the oxygen concentration decreased with time. At varying points of time, the medium was exchanged by fresh medium saturated with oxygen (Movie S1, ESI†). When the oxygen was fully depleted, the microcolonies disassembled (Fig. 1). We analysed the density of connected objects (element density) as a function of time. In the absence of oxygen, the bacteria moved as individual objects. When oxygen was supplied, the bacteria aggregated, reducing the density of connected objects (Fig. 1).

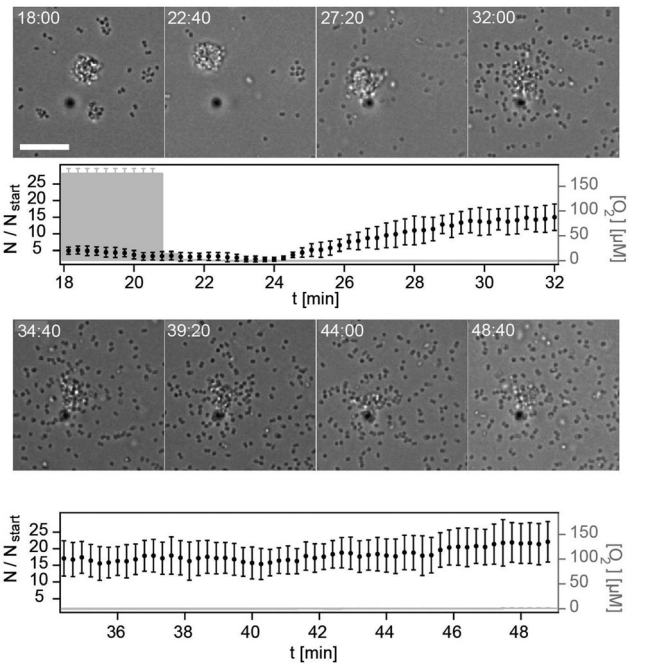

Fig. 1 Dynamics of gonococcal microcolonies during oxygen consumption. Gonococci were applied to the flow chamber and imaged at the PDMS surface with integrated oxygen sensor. In the beginning, the medium was saturated with oxygen. Bacteria rapidly depleted the oxygen. Top: time lapse microscopic images of gonoccci. Scale bar: 10 μm. Bottom: average relative element density N/N_{start} of 5 microcolonies (black circles, error bars: standard deviation of 5 colonies), oxygen concentration in medium (grey bars, error bars: calibration error of Stern–Volmer constant). This time series depicts a typical example from at least three independent experiments.

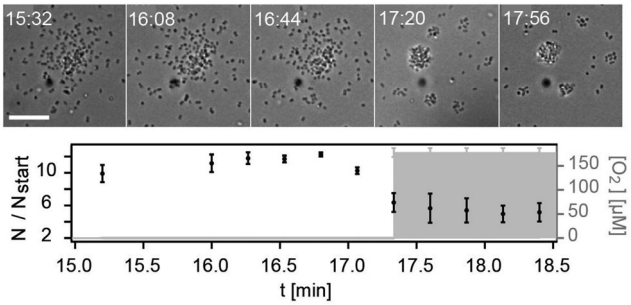

Fig. 2 Dynamics of gonococcal microcolonies during oxygen replenishment. Gonococci were applied to the flow chamber and imaged at the PDMS surface with integrated oxygen sensor. In the beginning, oxygen was depleted from the medium. After t = 16 min fresh medium saturated with oxygen was applied. Top: time lapse microscopic images of gonoccci. Scale bar: 10 µm. Bottom: average relative element density N/N_{start} of 5 microcolonies (black circles, error bars: standard deviation of 5 colonies), oxygen concentration in medium (grey bars, error bars: calibration error of Stern–Volmer constant). This time series depicts a typical example from at least three independent experiments.

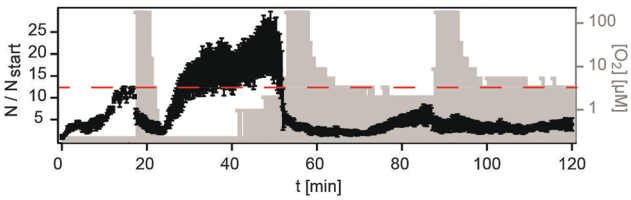

Fig. 3 Dynamics of gonococcal microcolonies. Gonococci were applied to the flow chamber and imaged at the PDMS surface with integrated oxygen sensor. In the beginning, microcolonies were present and had depleted the oxygen. At various time points fresh medium saturated with oxygen was supplied. Average relative element density N/N_{start} of 5 microcolonies (black circles, error bars: standard deviation of 5 colonies), oxygen concentration in medium (grey bars, error bars: calibration error of Stern–Volmer constant). Red dashed line: threshold concentration of oxygen for microcolony stability at $[O_2]$ = 3 µM. This time series depicts a typical example from at least three independent experiments.

Upon replenishment of oxygen with fresh oxygen-rich medium, microcolonies reformed within seconds (Fig. 2 and Movie S1, ESI†). Several cycles of colony dispersal upon oxygen depletion and colony formation upon replenishment were observed. The experiment shown in Fig. 3 started when colonies were formed and oxygen had just been depleted. While the colonies disintegrated the number of detected elements per area increased as more and more bacteria moved as individuals over the surface. After t = 16 min fresh medium saturated with oxygen was supplied and within seconds small microcolonies formed. Within minutes the oxygen concentration was again reduced to an undetectable level and the colonies disaggregated. Since the bacteria were able to multiply, the density of bacteria increased with time, explaining the increase in average density of elements from t = (17–50) min compared to the first cycle from t = (0–17) min. Repeated addition of fresh medium at t = 50 min, triggered re-formation of the microcolonies. Within minutes, oxygen levels were again strongly reduced, however a residual concentration of oxygen of $[O_2]$ = 3.3 µM was left in the medium. This very low concentration of

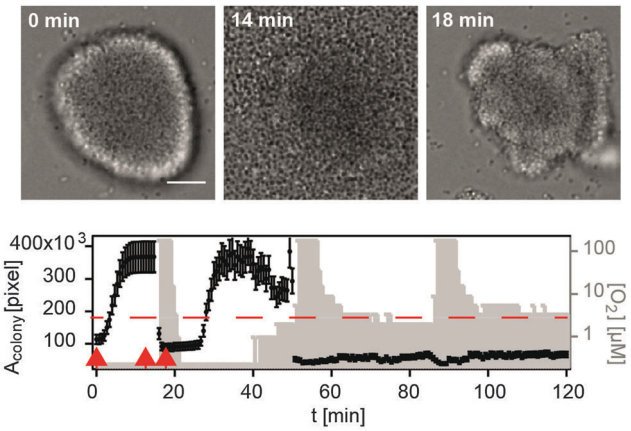

Fig. 4 Dynamics of large gonococcal microcolonies. Gonococci were applied to the flow chamber and imaged at the PDMS surface with integrated oxygen sensor. In the beginning, oxygen was depleted from the medium. Fresh medium saturated with oxygen was applied at various time points. Top: microscopic images of a typical large colony in the presence and absence of oxygen. Scale bar: 10 µm. Bottom: average relative area of microcolonies A_{colony} (black circles, error bars: standard deviation of 4 consecutive time points), oxygen concentration in medium (grey bars, error bars: calibration error of Stern–Volmer constant). The red arrows show the time points at which the images in (a) are taken. This time series depicts a typical example from at least three independent experiments.

oxygen was sufficient to keep the microcolonies assembled. We measured a threshold concentration of $[O_2]$ = 3 µM. When the oxygen concentration exceeded the threshold microcolonies were stable. Below the threshold microcolonies disassembled.

When the radius of the microcolonies exceeded $r \approx 7$ µm corresponding to ~1000 cells, they developed a kernel that showed strongly reduced mobility (Movie S2, ESI†). This kernel remained assembled upon depletion of oxygen (Fig. 4). Motile cells surrounded this kernel and left the dome-shaped microcolony in the absence of oxygen causing an increase in average area of the microcolonies. Here we analyzed the area of the colony instead of the density of elements since the concentration of cells surrounding the colony was too high to distinguish individual elements. Upon oxygen replenishment, these motile cells fused to the immobile kernels.

In conclusion, we showed that oxygen depletion triggers disassembly of early gonococcal microcolonies and oxygen replenishment triggers re-formation of the microcolonies within seconds.

Colony disassembly is an active process driven by type IV pilus retraction

We investigated whether disassembly of gonococcal microcolonies upon depletion of oxygen was an active process. We have shown previously, that gonococci use T4P-driven motility in the absence of oxygen and that the speed of surface motility is reduced ~2 fold. To assess the role of T4P retraction in the disassembly process, we inoculated bacteria that were deficient in T4P retraction. The respective strain ($pilT_{ind}$) carried the T4P retraction ATPase under the control of an inducible promoter. Since we did not induce expression of *pilT*, the gonococci

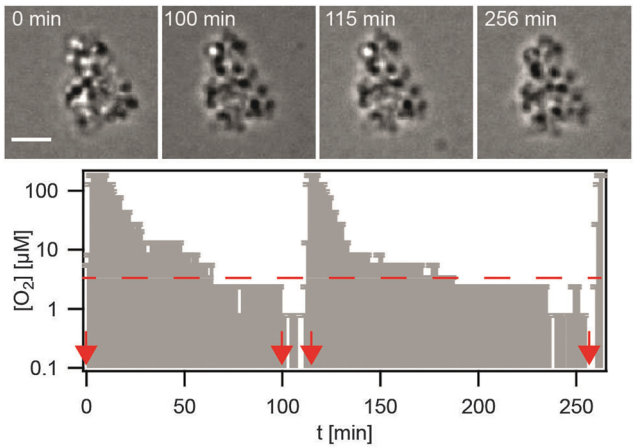

Fig. 5 Active T4P retraction is required for disassembly of microcolonies under anaerobic conditions. Retraction-deficient $pilT_{ind}$ gonococci were applied to the flow chamber and imaged at the PDMS surface with integrated oxygen sensor. Fresh medium saturated with oxygen was applied at various time points. Top: microscopic images of a typical colony in the presence and absence of oxygen. Scale bar: 5 μm. Bottom: concentration of oxygen as a function of time. The red dashed line denotes the minimal oxygen concentration necessary for microcolony stability. Arrows denote the time points at which the images shown were taken.

generated pili but were unable to retract them. As a consequence, the bacteria were not motile and formed large unstructured microcolonies[34] (Fig. 5 and Movie S3, ESI†). Such microcolonies were inoculated into the flow chamber. No disassembly or assembly dynamics was observed while oxygen was depleted or supplied (Movie S3, ESI†). When the *pilT* inducible strain was induced with 10 mM IPTG, PilT function was partially restored. Bacteria showed discontinuous motility. Under these conditions microcolonies dissociated partially when oxygen was depleted (Fig. S1, ESI†), confirming that active pilus retraction was required for disassembly of microcolonies.

We conclude that active T4P retraction is essential for the disassembly of the microcolonies upon depletion of oxygen.

Oxygen strongly enhances the pilus–pilus interaction force

We next assessed putative mechanisms that controlled cellular clustering *versus* adhesion to the surface. It was conceivable that the T4P–T4P interaction or the T4P–surface interaction was dependent on oxygen. In the first step, we tested T4P–T4P-interaction. To this end, we performed a crude pilus preparation under aerobic conditions.[35] The surface was then coated by pili and coating efficiency was verified by immunofluorescence. Subsequently, gonococci were inoculated and the reaction chamber was tightly sealed. While oxygen was present, bacteria formed microcolonies and exhibited twitching motility (Movie S4, ESI† and Fig. 6a). When oxygen was depleted, gonococci tended to desorb from the pilus-coated surface (Movie S5, ESI†). Fig. 6b shows several adhesion and desorption events. No microcolonies were found at the surface. We note that on uncoated glass surfaces gonococci adhere and move actively after oxygen depletion indicating that pilus-coating was responsible for inhibition of adherence and motility.[32]

In the next step, we trapped single gonococci in a laser trap maintaining them close to the T4P-coated surface. Due to the force applied by the optical trap, the cell body was maintained at the center of the trap. As the T4P bound to the surface and retracted, they exerted force on the cell body and the cell body was deflected from the center of the laser trap (Fig. 6c). This method allows measuring the frequency of T4P retractions of those pili that are attached to the surface (Fig. 6d). Under aerobic conditions 56% of 189 bacteria tested actively pulled with a frequency shown in Fig. 7b on the surface (Fig. 6e). Under anaerobic conditions only 2% of 194 tested bacteria pulled once on the surface (Fig. 6e).

Subsequently, we quantified the interaction force between T4P under aerobic conditions by comparing the distributions of maximum forces generated by gonococci onto a T4P-coated surface with the force generated onto a plain glass surface (Fig. 7a). Since the optical restoring force that pulls the bacterium into the center of the laser trap increases linearly with the deflection, the force pulling the bacterium into the trap increases with its excursion length from the center. Typically, an excursion ended when the pili pulling the cell forward detached from the surface and the bacterium moved rapidly back into the center of the trap (Fig. 6d). Since monococci (individual bacteria) and diplococci (two bacteria joined together), were considered, the error of the force measurement was on the order of 20% (Experimental).

We measured the maximum force that was generated by each pulling event prior to detachment of the pilus from the surface (Fig. 7a). On the uncoated glass surface the most likely maximum force was at $F \approx 10$ pN. Only 5% of the events exceeded $F = (25 \pm 5)$ pN (Fig. 7a). On the T4P-coated surface, gonococci generated considerably higher forces in the presence of oxygen. 65% of the events exceeded $F = (25 \pm 5)$ pN. While on the glass surface bacteria never escaped from the trap, on the pilus-coated surface, escaping bacteria were often observed indicating that they generated higher force. Using our setup, it was impossible to measure forces exceeding $F = (65 \pm 15)$ pN. For this reason all retraction events that generated forces exceeding 65 pN and all escape events were pooled into a single bin and shown at $F = 80$ pN. We did not attempt to measure the force generated by gonococci onto a pilus-coated surface under anaerobic conditions. Only 4 out of 194 bacteria tested showed a single retraction event, indicating that the pilus–pilus interaction force is too low for detection with our setup. The experiments demonstrate that in the presence of oxygen, T4P pili generated larger force on T4P than on glass surface. The frequencies at which the gonococci pulled out of the center of the trap were comparable between both conditions (Fig. 7b).

Finally, we tested whether the interaction force between T4P and glass increased under anaerobic conditions. We found no significant difference between the maximum force distributions under aerobic and anaerobic conditions (Fig. 7c). The frequencies at which the gonococci pulled out of the center of the trap were comparable between aerobic and anaerobic conditions

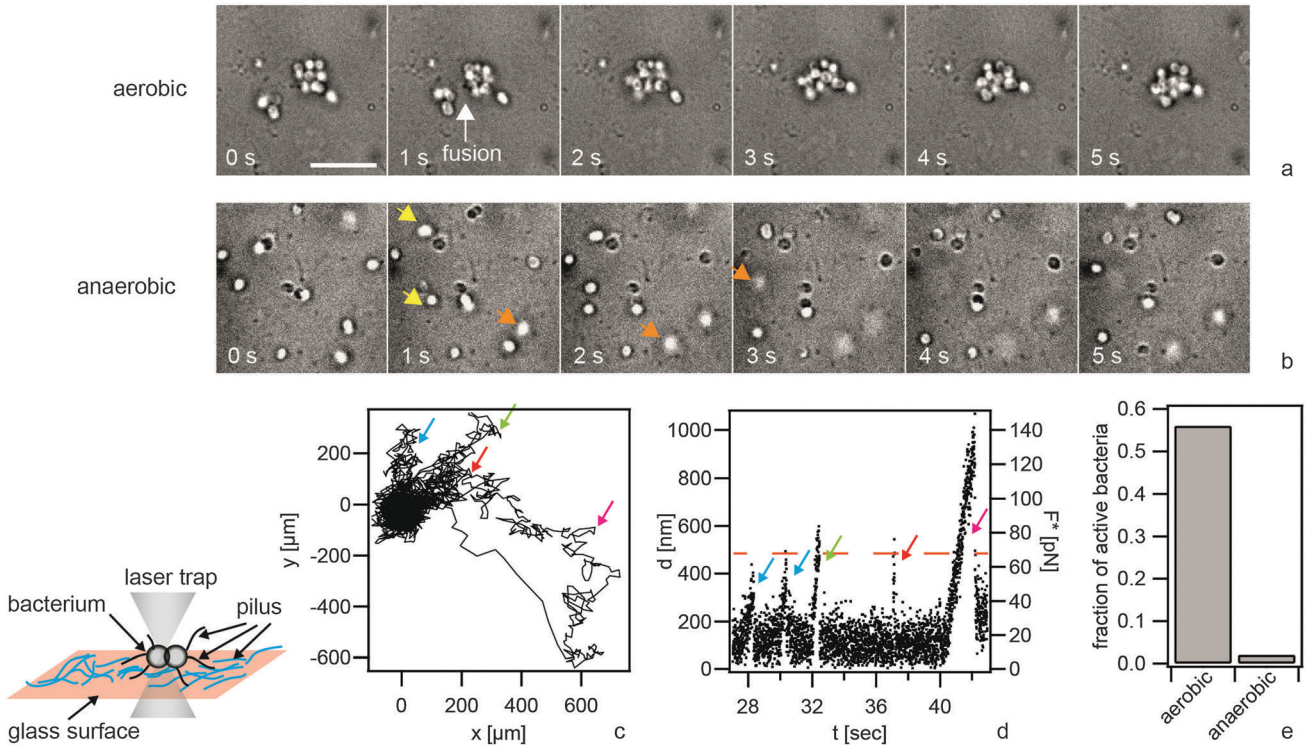

Fig. 6 Oxygen affects T4P–T4P interaction. Glass surfaces were coated with T4P harvested under aerobic conditions. Gonococci were inoculated and subsequently the chamber was sealed. Time lapse of gonococci on T4P-coated surface under (a) aerobic and (b) anaerobic conditions. Yellow arrows depict adsorption and orange arrows depict desorption of a bacterium. Scale bar: 5 μm. (c–e) A single gonococcus was trapped in an optical trap. Each deflection of the bacterial body from the center of the laser trap was registered. (c) Typical x–y trace of a single trapped gonococcus under aerobic conditions. (d) Corresponding deflection of the cell body from the center of the trap d as a function of time and force F^* exerted on the cell body by the trap. The dashed orange line at F^* = 65 pN denotes the force up to which force increases linearly with the deflection. Force measurement is not meaningful for $F^* > 65$ pN. Arrows denote retraction events. (e) Fraction of bacteria that actively pulled on the T4P-coated surface under aerobic and anaerobic conditions when trapped in a laser trap ($N > 184$ bacteria for each condition).

(Fig. 7d). We can therefore exclude the possibility that microcolonies disassemble at low O_2 concentrations because the interaction force with the glass surface is increased.

In conclusion, oxygen strongly enhances the T4P-mediated interaction between gonococci.

Depletion of proton motive force triggers colony disassembly

Oxygen is the final electron acceptor of the respiratory chain. It was therefore conceivable that depletion of proton motive force was the underlying mechanism for colony disassembly. To assess this hypothesis, we treated gonococcal microcolonies with the uncoupler carbonyl cyanide *m*-chlorophenyl hydrazone (CCCP) in the presence of oxygen. Gonococcal microcolonies disassembled in the presence of CCCP (Fig. 8). After removal of the drug the microcolonies re-formed. These experiments demonstrate that depletion of proton motive force triggers disassembly of microcolonies.

Chromosomal DNA stabilizes early microcolonies

We observed that large microcolonies do not disassemble fully. Since it is known that extracellular DNA supports early microcolony formation,[36] we addressed the question whether addition of chromosomal DNA stabilized early colonies. To this end, chromosomal DNA was added at a concentration of 0.78 μg ml^{-1} during inoculation of cells (Fig. 9 and Movie S6, ESI†). We found that the microcolonies were stable for at least one hour of sustained oxygen concentration below the threshold concentration of 3 μM. Replenishment of oxygen by addition of fresh medium with DNA did not significantly change the shape of the microcolonies.

In summary, application of chromosomal DNA stabilizes the microcolonies in the absence of oxygen.

Discussion

The surface properties and dynamics of type IV pili are crucial in determining bacterial interactions. Here, we have demonstrated that oxygen controls clustering of gonococci, most likely by controlling proton motive force. Mechanistically, we showed that the effect of oxygen on the stability of microcolonies stems from a change in the pilus–pilus interaction force.

It was also conceivable that the number of pili per cell, the speed of pilus retraction, the frequency of retractions, or force generation onto the surface or onto the body of adjacent cells were responsible for controlling the stability of the microcolonies in response to oxygen depletion. Recently, we have shown that the speed of single pilus retraction is lower by a

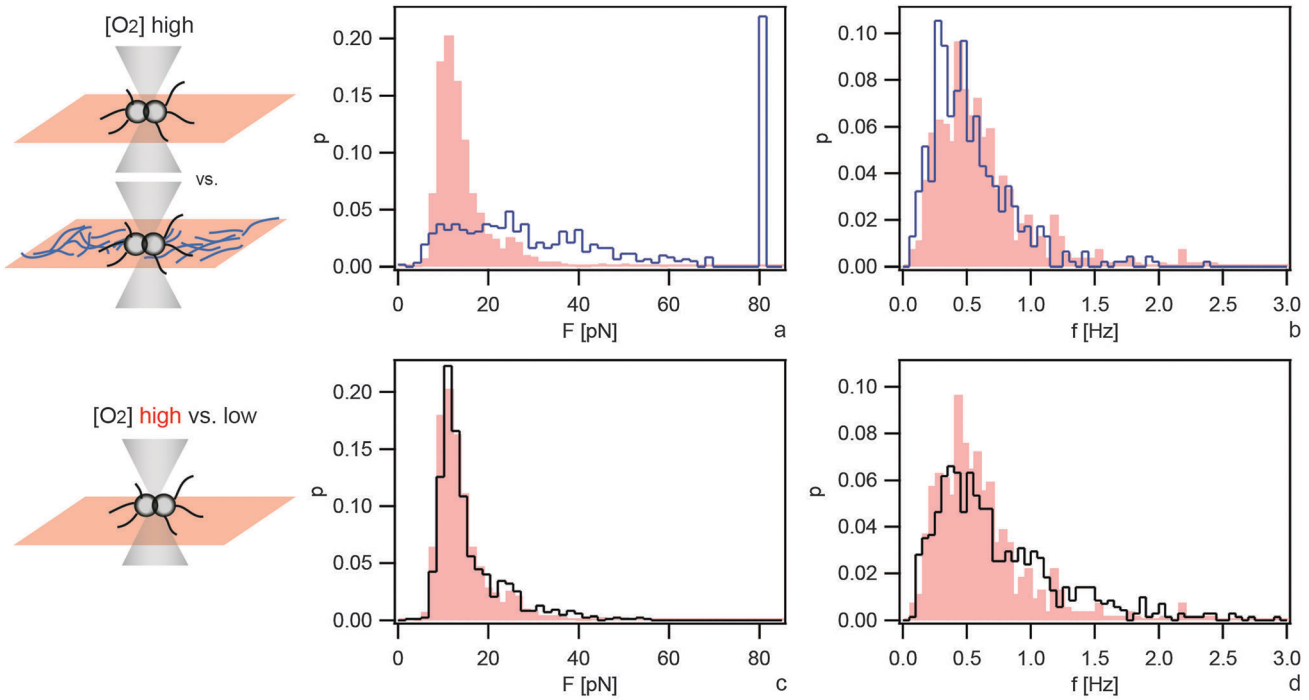

Fig. 7 T4P exert high force on other T4P. A single gonococcus was trapped in an optical trap. Each deflection of the bacterial body from the center of the laser trap was registered. (a) Distribution of maximum forces generated during individual deflection events under aerobic conditions, before the bacterium was pulled back to the center of the laser trap due to breakage of the bond between pili and the surface. Red bars: glass surface, blue line: T4P-coated surface. The single bar at F = 80 pN represents all events where F > 65 pN including escapes from the trap. (b) Distribution of retraction frequencies. Red bars: glass surface, blue line: T4P-coated surface. (c) Distribution of maximum forces generated during individual retraction events on a glass surface. Red bars: aerobic, black line: anaerobic. (d) Distribution of retraction frequencies. Red bars: aerobic, black line: anaerobic. (N > 600 retractions for each condition).

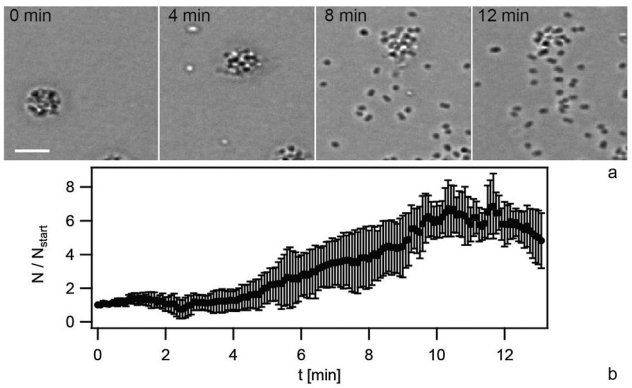

Fig. 8 Depletion of proton motive force triggers colony dissociation. Cells were inoculated into the flow chamber. Subsequently, a continuously flow of medium containing 50 μM CCCP was applied. (a) Time lapse of gonococcal microcolony. Scale bar: 5 μm. (b) Average relative element density of elements N/N_{start} (N = 4 colonies). This time series depicts a typical example from at least three independent experiments.

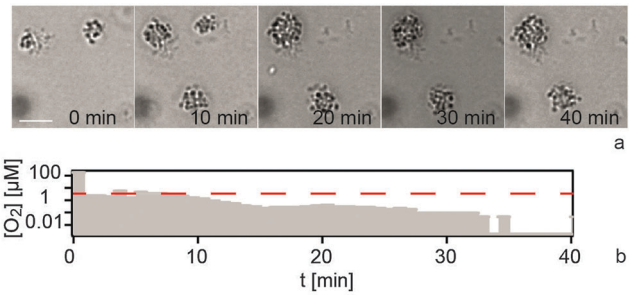

Fig. 9 Chromosomal DNA stabilizes microcolonies after oxygen depletion. Cells were inoculated in the presence of 0.78 μg ml^{-1} chromosomal DNA. Gonococci were imaged at the surface in the absence of flow and simultaneously the oxygen concentration was measured. (a) Time lapse of multiple microcolonies. Between 10 min and 20 min the upper colonies fused. Scale bar: 10 μm. (b) Concentration of oxygen as a function of time. The red dashed line denotes the minimal oxygen concentration necessary for microcolony stability in the absence of DNA in solution.

factor of ~2 and that the force generated by single pili is reduced under anaerobic conditions.[32,37] In this study, we investigated the role of oxygen on force generation by an entire cell by characterizing the force generated onto the surface. Using an inert glass surface, we found that the frequency of retraction events was hardly affected. The peak around 10 pN is in very good agreement with the force generated by single pili onto a glass bead.[11] Additionally it is in good agreement with the force measured onto the surface in a different medium.[38] If the underlying reason for disassembly of microcolonies was enhanced pilus–surface interaction under anaerobic conditions, then we would have expected that either the interaction force or the retraction frequency was significantly higher compared to

aerobic conditions. This prediction is not in agreement with our observations. Earlier studies on *P. aeruginosa* showed that when wt and pilin-deficient strains were mixed, motile wt bacteria formed the cap of mushroom-like structures.[39] These experiments suggest that *P. aeruginosa* use their pili for attachment to and motility along non-piliated bacteria. Here, we found that on the one hand microcolonies disassembled and on the other hand pilus–pilus interaction was virtually abolished under anaerobic conditions. We conclude that pilus–cell body interactions play only a minor role in this process.

By comparing the distribution of maximum forces between the T4P-coated surface and the glass surface we conclude that events generating forces exceeding F = 25 pN are almost exclusively caused by gonococcal T4P that bind T4P on the surface. More than 50% of all events detected generated $F >$ 25 pN. Therefore, we conclude that T4P–T4P interaction forces strongly exceed the force that T4P exert onto a glass surface. We note, however, that we were unable to characterize the distribution of forces generated between gonococci and T4P in a quantitative manner because the force generated by the bacteria onto the T4P-coated surface often exceeded the linear range of the optical trap.

Strikingly, the interaction between gonococci and a T4P-coated surface was severely inhibited under anaerobic conditions. This clearly demonstrates that pilus–pilus interactions and not the dynamics of T4P are responsible for the disassembly of microcolonies under anaerobic conditions. The pilus–pilus interaction may be influenced by several factors. One prominent molecular mechanism for altering their interaction is post-translational modification of the major pilin PilE. Glycosylation or phosphoform-modifications are likely to influence pilus–pilus interactions. Wt (N400) gonococci usually bear a disaccharide composed of a hexose residue linked to a proximal 2,4-diacetamino-2,4,6-trideoxyhexose (HexDATDH) at serine 63.[18] The product of *pglE* is responsible for generating trisaccharide modifications of pilin.[40] As *pglE* is phase-variable, *i.e.* it can switch between an expressed and a silent state, gonococci may have different pilin glycosilation forms. Furthermore, pilin can be modified with phosphatidylethonolamine (PE).[18] In *N. meningiditis* pilin phosphotransferase PptB was shown to be upregulated during infection leading to decomposition of microcolonies and migration through an endothelial cell layer.[19] In particular, modelling of antiparallel structures of T4P predicted that addition of phosphoglycerol strongly destabilizes the formation of pilus-bundles. We hypothesize that the state of post-translational modification of T4P may respond to the oxygen concentration within seconds.

Another molecular mechanism that influences pilus-mediated interactions is the presence of minor pilins. Minor pilins have a similar structure compared to the major pilin PilE but are generated at lower levels. It is still not fully clear, which of the minor pilins are integrated into the pilus-fibre. While earlier studies supported the idea that minor pilins are integrated into the pilus,[15,41] more recent experiments suggest that not all of them are integrated but remain in the cytoplasmic membrane, without losing their functionality.[42] No matter where they are located, they strongly influence pilus-interactions. Deletion of gonocccal *pilH* (or menigococcal *pilX*) reduces T4P number to a very low level.[16,42] Deletion of *pilI*, *J*, *K*, *L* generates unpiliated gonococci, but additional deletion of *pilT* restores piliation.[16] We can exclude that any of these minor pilin PilH through PilL are the major players in our study since gonococci are motile on glass both under aerobic and under anaerobic conditions the indicating that piliation is not affected strongly.[11] More importantly, the minor pilins PilV and ComP have a minor effect on the level of piliation but affect DNA binding and uptake severely.[13,14] PilV strongly reduces the amount of DNA imported into the periplasm by acting antagonistically on ComP. On the other hand, PilV supports adhesion to host cells.[14,43,44] We have shown that addition of extracellular DNA stabilizes microcolonies under anaerobic conditions. Since ComP is important for pilus-dependent binding of DNA[45] it may be involved in the stability of the microcolony.

N. gonorrhoeae carry an oxygen sensing system. Gene expression in response to oxygen is regulated by the transcriptional activator FNR, which senses oxygen by direct binding and activates the truncated denitrification pathway when oxygen becomes limited.[46–48] Moreover, when *N. gonorrhoeae* is grown anaerobically, the level of piliation is reduced since *pilC2* expression is down-regulated.[49] In our study, we observed that microcolonies formed within seconds after oxygen replenishment. This response is much faster than a process that requires gene expression. However, the oxygen sensor FNR may have a second function in protein interactions. Taken together, we propose that rapid activation or deactivation of a protein that controls either the post-translational modification of pilin or the function of the minor pilins are most likely responsible for the change of pilus–pilus interaction strength in response to oxygen limitation.

Previously we proposed that reduction of the speed of surface motility under anaerobic conditions may promote biofilm formation.[32] Our idea was that oxygen gradients form in microcolonies generating less motile cells in the center of a biofilm. Our present study shows that the opposite is true; oxygen depletion causes disassembly of microlonies. Potentially, gonococci increase their surface area in response to oxygen limitation to enable better access to residual oxygen or other sources of nutrients.

Conclusion

N. gonorrhoeae has been co-isolated with obligate anaerobic bacteria and recently it has been shown that it can grow under anaerobic conditions using a truncated denitrification pathway. Here, we demonstrated that fluctuating oxygen concentrations rapidly induce assembly and disassembly of gonococcal microcolonies. Mechanistically, the strength of pilus–pilus interaction responds to oxygen depletion. In future experiments it will be interesting to find the molecular players that change these interaction forces.

Experimental

Bacterial strains and growth conditions

We used two derivatives of MS11. Strain N400 carried an IPTG-inducible $recA_{ind}$ copy.[50,51] RecA does not influence T4P dynamics, but inhibits pilin antigenic variation. This strain was used for the experiments unless otherwise noted. Furthermore, an IPTG-inducible $pilT_{ind}$ strain in the $recA_{ind}$ background was used.[52] *N. gonorrhoeae* was grown overnight at 37 °C and 5% CO_2 on agar plates containing gonococcal base agar 10 g l^{-1} Bacto™ agar (BD Biosciences, Bedford, MA, USA), 5 g l^{-1} NaCl (Roth, Darmstadt, Germany), 4 g l^{-1} K_2HPO_4 (Roth), 1 g l^{-1} KH_2PO_4 (Roth), 15 g l^{-1} Bacto™ Proteose Peptone No. 3 (BD), 0.5 g l^{-1} soluble starch (Sigma-Aldrich, St. Louis, MO, USA) and the following supplements: 1 g l^{-1} D-glucose (Roth), 0.1 g l^{-1} L-glutamine (Roth), 0.289 g l^{-1} L-cysteine-HCL × H_2O (Roth), 1 mg l^{-1} thiamine pyrophosphate (Sigma-Aldrich), 0.2 mg l^{-1} $Fe(NO_3)_3$ (Sigma-Aldrich), 0.03 mg l^{-1} thiamine HCl (Roth), 0.13 mg l^{-1} 4-aminobenzoic acid (Sigma-Aldrich), 2.5 mg l^{-1} β-nicotinamide adenine dinucleotide (Roth) and 0.1 mg l^{-1} vitamin B_{12} (Sigma-Aldrich). Before each experiment gonococcal colonies were resuspended in GC-medium.

Measurement of oxygen concentration

Measurement of oxygen concentration has been described in detail in Kurre & Maier.[32] In short, an oxygen sensor based on the oxygen sensitive dye Pt(II) *meso*-tetra(pentafluorophenyl)porphine PtTFPP (Frontier Scientific, Logan, Utah, USA) was fabricated to monitor oxygen consumption and bacterial motility simultaneously.[53] Stock solution of PtTFPP (20 mM in toluene) was stored at RT. PtTFPP is embedded in a Sylgard 184 polydimethylsiloxane network (PDMS, Dow Corning, Midland, Michigan, USA). Therefore, PDMS was mixed with Sylgard 184 curing agent (ratio 10 : 1) and 1 mM PtTFPP and directly spin-coated on cover slides to result in ∼30 μm thin layers. In the end, oxygen sensors were cured at 60 °C for at least 3 hours. Calibration and oxygen measurements are described in.[32] Images for oxygen measurements were taken every 30 s at a distance of 1 mm away from the site where the microcolony dynamics was imaged to avoid photodamage.

Surface coating with T4P

Type IV pili were purified according to a method described by Brinton *et al.*[54] In short, bacteria were solubilized in 150 mM ethanolamine buffer pH 10.5. T4P were sheared off by vigorous vortexing. Bacteria were centrifuged and 10% saturated ammonium sulfate was added to the supernatant. The supernatant was incubated for 30 min at room temperature and subsequently centrifuged to collect the pili. The pellet was washed in TBS pH 8.0 and stored in ddH_2O at −20 °C.

Microscopy

A homemade flow chamber was mounted into an inverted microscope (Nikon TI). It consists of a Teflon construction where a single channel (length: 56 mm, width: 6 mm, height: 1 mm) was fabricated by adding a cover slide on top and a cover slide coated with the oxygen sensor at the bottom of this construction. Glass slides were sealed with picodent twinsil (Picodent). A single inlet and outlet allowed for exchanging the medium using a peristaltic pump.

Image analysis

We used Matlab with the dipimage toolbox to analyse the microscopy images. The selected region of interest of every single image was edited with a band pass filter to create a binary image. Of the calculated local variance image the holes of enclosed areas were filled and defined as a single element. In the presence of oxygen, a region of interest was defined around a single microcolony. The number of elements within this area was defined as the element density. We normalized the element density to the element density at the start of the experiment, yielding. From this the average relative area of microcolonies and the element density of connected objects N/N_{start} as a function of time could be calculated.

Retraction force measurement. The optical tweezers were assembled on a Zeiss Axiovert 200 microscope as described previously.[30] The assay was modified for measuring the force generated by a single surface-attached bacterium as a function of time.[38] The trap was calibrated by spectrum analysis of Brownian motion of individual monococci and was found to have a stiffness of 0.14 pN nm^{-1} ± 10%. The position of trapped bacteria was detected at 20 kHz using a quadrant photodiode and the sample stage was movable *via* a combined piezo and electric motor.

Using the traction force method, we found that the linear range of the optical trap was d = 450 nm when gonococci were trapped. Therefore the maximum force we detected was F = 65 pN. Gonococci often form diplococci, *i.e.* two bacteria are joined together. In the optical trap, diplococci line up with their major axis parallel to the optical axis. At the surface, however, diplococci sometimes pull themselves into a position where their major axis is perpendicular to the optical axis. This rotation of the major axis affects the signal detected by the quadrant photodiode. We estimate the error 20% on the force detected. Although this error is large, it equally affects interactions between bacteria and surface under different conditions. Therefore the distributions of maximum forces can be directly compared.

The retraction experiments were performed in a sealed chamber using a low density suspension of N400, allowing for undisturbed measurement of single bacteria over a period of minutes. During the experiment, a single bacterium was trapped near the surface using the optical tweezers. Retraction of surface-bound pili resulted in deflection of the bacterium from the center of the optical trap as measured by the four-quandrand photodiode. The force acting on a bacterium is proportional to this deflection and was calculated using the calibration described above. After several minutes, a detrimental effect of the optical trap on the bacterium became apparent and it was abandoned.

Acknowledgements

We thank Rainer Kurre, Philip Valerius, and Claudia Meel for helpful discussions and experimental support. In particular, we

are grateful to Enno Oldewurtel for providing us with his improved flow cell. This project was funded by the Deutsche Forschungsgemeinschaft through grant MA 3898.

Notes and references

1 O. E. Petrova and K. Sauer, *J. Bacteriol.*, 2012, **194**, 2413–2425.
2 R. S. Friedlander, H. Vlamakis, P. Kim, M. Khan, R. Kolter and J. Aizenberg, *Proc. Natl. Acad. Sci. U. S. A.*, 2013, **110**, 5624–5629.
3 K. M. Blair, L. Turner, J. T. Winkelman, H. C. Berg and D. B. Kearns, *Science*, 2008, **320**, 1636–1638.
4 G. A. O'Toole and R. Kolter, *Mol. Microbiol.*, 1998, **30**, 295–304.
5 J. C. Conrad, *Res. Microbiol.*, 2012, **163**, 619–629.
6 K. Zhao, B. S. Tseng, B. Beckerman, F. Jin, M. L. Gibiansky, J. J. Harrison, E. Luijten, M. R. Parsek and G. C. Wong, *Nature*, 2013, **497**, 388–391.
7 S. Wang, M. R. Parsek, D. J. Wozniak and L. Z. Ma, *Environ. Microbiol.*, 2013, **15**, 2238–2253.
8 E. S. Gloag, L. Turnbull, A. Huang, P. Vallotton, H. Wang, L. M. Nolan, L. Mililli, C. Hunt, J. Lu, S. R. Osvath, L. G. Monahan, R. Cavaliere, I. G. Charles, M. P. Wand, M. L. Gee, R. Prabhakar and C. B. Whitchurch, *Proc. Natl. Acad. Sci. U. S. A.*, 2013, **110**, 11541–11546.
9 C. L. Giltner, Y. Nguyen and L. L. Burrows, *Microbiol. Mol. Biol. Rev.*, 2012, **76**, 740–772.
10 L. Craig, R. K. Taylor, M. E. Pique, B. D. Adair, A. S. Arvai, M. Singh, S. J. Lloyd, D. S. Shin, E. D. Getzoff, M. Yeager, K. T. Forest and J. A. Tainer, *Mol. Cell*, 2003, **11**, 1139–1150.
11 C. Holz, D. Opitz, L. Greune, R. Kurre, M. Koomey, M. A. Schmidt and B. Maier, *Phys. Rev. Lett.*, 2010, **104**, 178104.
12 L. Craig and J. Li, *Curr. Opin. Struct. Biol.*, 2008, **18**, 267–277.
13 F. E. Aas, M. Wolfgang, S. Frye, S. Dunham, C. Lovold and M. Koomey, *Mol. Microbiol.*, 2002, **46**, 749–760.
14 F. E. Aas, C. Lovold and M. Koomey, *Mol. Microbiol.*, 2002, **46**, 1441–1450.
15 S. Helaine, D. H. Dyer, X. Nassif, V. Pelicic and K. T. Forest, *Proc. Natl. Acad. Sci. U. S. A.*, 2007, **104**, 15888–15893.
16 H. C. Winther-Larsen, M. Wolfgang, S. Dunham, J. P. van Putten, D. Dorward, C. Lovold, F. E. Aas and M. Koomey, *Mol. Microbiol.*, 2005, **56**, 903–917.
17 C. Vink, G. Rudenko and H. S. Seifert, *FEMS Microbiol. Rev.*, 2012, **36**, 917–948.
18 F. T. Hegge, P. G. Hitchen, F. E. Aas, H. Kristiansen, C. Lovold, W. Egge-Jacobsen, M. Panico, W. Y. Leong, V. Bull, M. Virji, H. R. Morris, A. Dell and M. Koomey, *Proc. Natl. Acad. Sci. U. S. A.*, 2004, **101**, 10798–10803.
19 J. Chamot-Rooke, G. Mikaty, C. Malosse, M. Soyer, A. Dumont, J. Gault, A. F. Imhaus, P. Martin, M. Trellet, G. Clary, P. Chafey, L. Camoin, M. Nilges, X. Nassif and G. Dumenil, *Science*, 2011, **331**, 778–782.
20 F. Miller, G. Phan, T. Brissac, C. Bouchiat, G. Lioux, X. Nassif and M. Coureuil, *mBio*, 2014, **5**, e01024.
21 B. Maier, L. Potter, M. So, C. D. Long, H. S. Seifert and M. P. Sheetz, *Proc. Natl. Acad. Sci. U. S. A.*, 2002, **99**, 16012–16017.
22 M. Clausen, V. Jakovljevic, L. Sogaard-Andersen and B. Maier, *J. Bacteriol.*, 2009, **191**, 4633–4638.
23 B. Maier, *Soft Matter*, 2013, **9**, 5667–5671.
24 M. Wolfgang, P. Lauer, H. S. Park, L. Brossay, J. Hebert and M. Koomey, *Mol. Microbiol.*, 1998, **29**, 321–330.
25 A. J. Merz, M. So and M. P. Sheetz, *Nature*, 2000, **407**, 98–102.
26 J. M. Skerker and H. C. Berg, *Proc. Natl. Acad. Sci. U. S. A.*, 2001, **98**, 6901–6904.
27 R. Marathe, C. Meel, N. C. Schmidt, L. Dewenter, R. Kurre, L. Greune, M. A. Schmidt, M. J. Muller, R. Lipowsky, B. Maier and S. Klumpp, *Nat. Commun.*, 2014, **5**, 3759.
28 V. Zaburdaev, N. Biais, M. Schmiedeberg, J. Eriksson, A. B. Jonsson, M. P. Sheetz and D. A. Weitz, *Biophys. J.*, 2014, **107**, 1523–1531.
29 C. Holz, D. Opitz, J. Mehlich, B. J. Ravoo and B. Maier, *Nano Lett.*, 2009, **9**, 4553–4557.
30 M. Clausen, M. Koomey and B. Maier, *Biophys. J.*, 2009, **96**, 1169–1177.
31 B. Maier, M. Koomey and M. P. Sheetz, *Proc. Natl. Acad. Sci. U. S. A.*, 2004, **101**, 10961–10966.
32 R. Kurre and B. Maier, *Biophys. J.*, 2012, **102**, 2556–2563.
33 R. Kurre, N. Kouzel, K. Ramakrishnan, E. R. Oldewurtel and B. Maier, *PLoS One*, 2013, **8**, e67718.
34 D. L. Higashi, G. H. Zhang, N. Biais, L. R. Myers, N. J. Weyand, D. A. Elliott and M. So, *Microbiology*, 2009, **155**, 4084–4092.
35 D. Opitz and B. Maier, *PLoS One*, 2011, **6**, e17088.
36 M. Zweig, S. Schork, A. Koerdt, K. Siewering, C. Sternberg, K. Thormann, S. V. Albers, S. Molin and C. van der Does, *Environ. Microbiol.*, 2014, **16**, 1040–1052.
37 R. Kurre, A. Hone, M. Clausen, C. Meel and B. Maier, *Mol. Microbiol.*, 2012, **86**, 857–865.
38 M. T. Anderson, L. Dewenter, B. Maier and H. S. Seifert, *mBio*, 2014, **5**, e01004.
39 M. Klausen, A. Aaes-Jorgensen, S. Molin and T. Tolker-Nielsen, *Mol. Microbiol.*, 2003, **50**, 61–68.
40 F. E. Aas, A. Vik, J. Vedde, M. Koomey and W. Egge-Jacobsen, *Mol. Microbiol.*, 2007, **65**, 607–624.
41 C. L. Giltner, M. Habash and L. L. Burrows, *J. Mol. Biol.*, 2010, **398**, 444–461.
42 A. F. Imhaus and G. Dumenil, *EMBO J.*, 2014, **33**, 1767–1783.
43 H. Gangel, C. Hepp, S. Muller, E. R. Oldewurtel, F. E. Aas, M. Koomey and B. Maier, *PLoS Pathog.*, 2014, **10**, e1004043.
44 H. C. Winther-Larsen, F. T. Hegge, M. Wolfgang, S. F. Hayes, J. P. van Putten and M. Koomey, *Proc. Natl. Acad. Sci. U. S. A.*, 2001, **98**, 15276–15281.
45 A. Cehovin, P. J. Simpson, M. A. McDowell, D. R. Brown, R. Noschese, M. Pallett, J. Brady, G. S. Baldwin, S. M. Lea, S. J. Matthews and V. Pelicic, *Proc. Natl. Acad. Sci. U. S. A.*, 2013, **110**, 3065–3070.
46 V. L. Clark, V. Isabella, K. Barth and C. Overton, *Regulation and Function of the Neisserial Denitrification Pathway*, Caister Academic Press, 2010.
47 S. Lissenden, S. Mohan, T. Overton, T. Regan, H. Crooke, J. A. Cardinale, T. C. Householder, P. Adams, C. D. O'Conner,

V. L. Clark, H. Smith and J. A. Cole, *Mol. Microbiol.*, 2000, **37**, 839–855.

48 R. N. Whitehead, T. W. Overton, L. A. Snyder, S. J. McGowan, H. Smith, J. A. Cole and N. J. Saunders, *BMC Genomics*, 2007, **8**, 35.

49 J. Mellies, T. Rudel and T. F. Meyer, *Mol. Gen. Genet.*, 1997, **255**, 285–293.

50 H. S. Seifert, *Gene*, 1997, **188**, 215–220.

51 T. Tonjum, N. E. Freitag, E. Namork and M. Koomey, *Mol. Microbiol.*, 1995, **16**, 451–464.

52 M. Wolfgang, H. S. Park, S. F. Hayes, J. P. van Putten and M. Koomey, *Proc. Natl. Acad. Sci. U. S. A.*, 1998, **95**, 14973–14978.

53 P. C. Thomas, M. Halter, A. Tona, S. R. Raghavan, A. L. Plant and S. P. Forry, *Anal. Chem.*, 2009, **81**, 9239–9246.

54 C. Brinton, J. Bryan, J. Dillon, L. Jacobson, A. Labik, S. Lee, A. Levine, S. Lim, J. McMichael, S. Polen, K. Rogers, A. To and S. To, *Uses of pili in gonorrhea control: role of bacterial pili in disease, purification and properties of gonococcal pili, and progress in the development of a gonococcal pilus vaccine for gonorrhea*, ASM, Washington, DC, 1978.

